Search for the Decays $B_s^0 \to \tau^+\tau^-$ and $B^0 \to \tau^+\tau^-$

R. Aaij *et al.*[*]
(LHCb Collaboration)

(Received 13 March 2017; revised manuscript received 25 April 2017; published 21 June 2017)

A search for the rare decays $B_s^0 \to \tau^+\tau^-$ and $B^0 \to \tau^+\tau^-$ is performed using proton–proton collision data collected with the LHCb detector. The data sample corresponds to an integrated luminosity of 3 fb^{-1} collected in 2011 and 2012. The τ leptons are reconstructed through the decay $\tau^- \to \pi^-\pi^+\pi^-\nu_\tau$. Assuming no contribution from $B^0 \to \tau^+\tau^-$ decays, an upper limit is set on the branching fraction $\mathcal{B}(B_s^0 \to \tau^+\tau^-) < 6.8 \times 10^{-3}$ at the 95% confidence level. If instead no contribution from $B_s^0 \to \tau^+\tau^-$ decays is assumed, the limit is $\mathcal{B}(B^0 \to \tau^+\tau^-) < 2.1 \times 10^{-3}$ at the 95% confidence level. These results correspond to the first direct limit on $\mathcal{B}(B_s^0 \to \tau^+\tau^-)$ and the world's best limit on $\mathcal{B}(B^0 \to \tau^+\tau^-)$.

DOI: 10.1103/PhysRevLett.118.251802

Processes where a B meson decays into a pair of oppositely charged leptons are powerful probes in the search for physics beyond the Standard Model (SM). Recently, the first observation of the $B_s^0 \to \mu^+\mu^-$ decay was made [1,2] (the inclusion of charge-conjugate processes is implied throughout this Letter). Its measured branching fraction ($\mathcal{B}$) is compatible with the SM prediction [3] and imposes stringent constraints on theories beyond the SM. Complementing this result with searches for the tauonic modes $B \to \tau^+\tau^-$, where B can be either a B^0 or a B_s^0 meson, is of great interest in view of the recent hints of lepton flavor nonuniversality obtained by several experiments. In particular the measurements of $R(D^{(*)}) = [\mathcal{B}(B^0 \to D^{(*)}\tau^+\nu_\tau)]/[\mathcal{B}(B^0 \to D^{(*)}\ell^+\nu_\ell)]$, where ℓ^+ represents either a muon, an electron or both, are found to be larger than the SM prediction by 3.9 standard deviations (σ) [4], and the measurement of $R_K = [\mathcal{B}(B^+ \to K^+\mu^+\mu^-)]/[\mathcal{B}(B^+ \to K^+e^+e^-)]$ is 2.6σ lower than the SM prediction [5]. Possible explanations for these and other [6] deviations from their SM expectations include leptoquarks, W'/Z' bosons, and two-Higgs-doublet models (see, e.g., Refs. [7,8]). In these models, the $B \to \tau^+\tau^-$ branching fractions could be enhanced with respect to the SM predictions, $\mathcal{B}(B^0 \to \tau^+\tau^-) = (2.22 \pm 0.19) \times 10^{-8}$ and $\mathcal{B}(B_s^0 \to \tau^+\tau^-) = (7.73 \pm 0.49) \times 10^{-7}$ [3], by several orders of magnitude [8–12]. All minimal-flavor-violating models predict the same enhancement of $\mathcal{B}(B_s^0 \to \tau^+\tau^-)$ over $\mathcal{B}(B^0 \to \tau^+\tau^-)$ as in the SM.

The experimental search for $B \to \tau^+\tau^-$ decays is complicated by the presence of at least two undetected neutrinos, originating from the decay of the τ leptons. The *BABAR* collaboration has searched for the $B^0 \to \tau^+\tau^-$ mode [13] and published an upper limit $\mathcal{B}(B^0 \to \tau^+\tau^-) < 4.10 \times 10^{-3}$ at the 90% confidence level (C.L.). There are currently no experimental results for the $B_s^0 \to \tau^+\tau^-$ mode, though its branching fraction can be indirectly constrained to be less than 3% at the 90% C.L. [14–16].

In this Letter, the first search for the rare decay $B_s^0 \to \tau^+\tau^-$ is presented, along with a search for the $B^0 \to \tau^+\tau^-$ decay. The analysis is performed with proton–proton collision data corresponding to integrated luminosities of 1.0 and 2.0 fb^{-1} recorded with the LHCb detector at center-of-mass energies of 7 and 8 TeV, respectively. The τ leptons are reconstructed through the decay $\tau^- \to \pi^-\pi^+\pi^-\nu_\tau$, which proceeds predominantly through the decay chain $\tau^- \to a_1(1260)^-\nu_\tau$, $a_1(1260)^- \to \rho(770)^0\pi^-$ [17]. The branching fraction $\mathcal{B}(\tau^- \to \pi^-\pi^+\pi^-\nu_\tau)$ is $(9.31 \pm 0.05)\%$ [18]. Because of the final-state neutrinos, the $\tau^+\tau^-$ mass provides only a weak discrimination between signal and background, and cannot be used as a way to distinguish B_s^0 from B^0 decays. The number of signal candidates is obtained from a fit to the output of a multivariate classifier that uses a range of kinematic and topological variables as input. Data-driven methods are used to determine signal and background models. The observed signal yield is converted into a branching fraction using as a normalization channel the decay $B^0 \to D^-D_s^+$ [19,20], with $D^- \to K^+\pi^-\pi^-$ and $D_s^+ \to K^-K^+\pi^+$.

The LHCb detector, described in detail in Refs. [21,22], is a single-arm forward spectrometer covering the pseudorapidity range $2 < \eta < 5$. The online event selection is performed by a trigger [23], which consists of a hardware stage, based on information from the calorimeter and muon systems, followed by a software stage, which applies a full event reconstruction. The hardware trigger stage requires events to have a muon with high transverse momentum (p_T) with respect to the beam line or a hadron, photon, or electron

[*]Full author list given at the end of the article.

with high transverse energy in the calorimeters. For hadrons, the transverse energy threshold is around 3.5 GeV, depending on the data-taking conditions. The software trigger requires a two-, three-, or four-track secondary vertex with a significant displacement from the primary pp interaction vertices (PVs). A multivariate classifier [24] is used for the identification of secondary vertices that are significantly displaced from the PVs, and are consistent with the decay of a b hadron. At least one charged particle must have $p_T > 1.7$ GeV/c and be inconsistent with originating from any PV.

Simulated data are used to optimize the selection, obtain the signal model for the fit and determine the selection efficiencies. In the simulation, pp collisions are generated using PYTHIA [25] with a specific LHCb configuration [26]. Decays of hadrons are described by EVTGEN [27], in which final-state radiation is generated using PHOTOS [28]. The interaction of the generated particles with the detector, and its response, are implemented using the GEANT4 toolkit [29] as described in Ref. [30]. The $\tau^- \to \pi^-\pi^+\pi^-\nu_\tau$ decays are generated using the resonance chiral Lagrangian model [31] with a tuning based on the *BABAR* results for the $\tau^- \to \pi^-\pi^+\pi^-\nu_\tau$ decays [32], implemented in the TAUOLA generator [33].

In the off-line selection of the candidate signal and normalization decays, requirements on the particle identification (PID) [34], track quality, and the impact parameter with respect to any PV are imposed on all charged final-state particles. Three charged tracks, identified as pions for the $B \to \tau^+\tau^-$ decays, and pions or kaons for the $B^0 \to D^-D_s^+$ decays, forming a good-quality vertex are combined to make intermediate τ, D^+, and D_s^+ candidates. The kinematic properties of these candidates, like momenta and masses, are calculated from the three-track combinations. The flight directions of the τ, D^+, and D_s^+ candidates are estimated from their calculated momentum vectors. For the τ candidates this is a biased estimate due to the missing neutrinos. In turn, B-meson candidates are reconstructed from two oppositely charged τ or from D^- and D_s^+ candidates with decay vertices well separated from the PVs. The B-meson candidates are required to have $p_T > 2$ GeV/c, at least one τ, D^+, and D_s^+ candidate with $p_T > 4$ GeV/c and at least one pion or kaon with $p_T > 2$ GeV/c. No further selection requirements are imposed on the normalization mode.

For each τ candidate, the two-dimensional distribution of the invariant masses $m_{\pi^+\pi^-}$ of the two oppositely charged two-pion combinations is divided into nine sectors, as illustrated in Fig. 1. Exploiting the intermediate $\rho(770)^0$ resonance of the τ decays, these sectors are used to define three regions. The signal region consists of B candidates with both τ candidates in sector 5, and is used to determine the signal yield. The signal-depleted region, composed of B candidates having at least one τ candidate in sectors 1, 3, 7, or 9, provides a sample used when optimizing the selection.

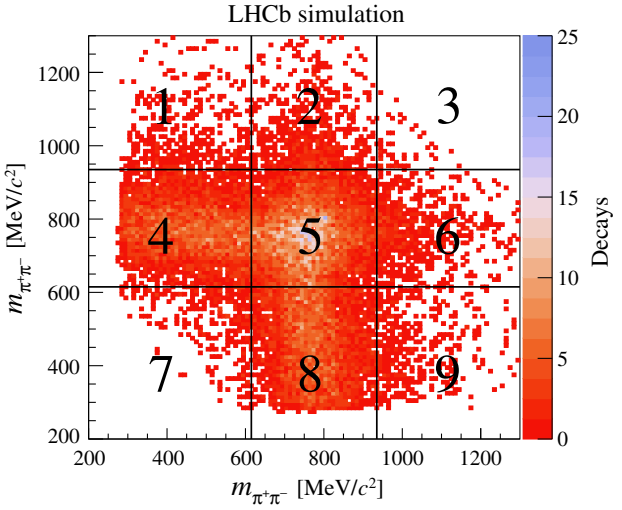

FIG. 1. Two-dimensional distribution of the invariant masses $m_{\pi^+\pi^-}$ of the two oppositely charged two-pion combinations for simulated $B_s^0 \to \tau^+\tau^-$ candidates. The distribution is symmetric by construction. The vertical and horizontal lines illustrate the sector boundaries.

The control region corresponds to B candidates with one τ candidate in sectors 4, 5, or 8 and the other in sectors 4 or 8, and provides the background model.

For the $B \to \tau^+\tau^-$ modes, further requirements are imposed on two types of isolation variables that are able to discriminate signal from background from partially reconstructed decays with additional charged or neutral particles. The first class of isolation variables, based on the decision of a multivariate classifier trained on simulated signal and other b-hadron decays, discriminates against processes containing additional charged tracks that either make a good-quality vertex with any selected pion or τ candidate, or belong to the same b-hadron decay as the selected pion candidates. The second class of isolation variables is based on calorimeter activity due to neutral particles in a cone, defined in terms of the pseudorapidity and polar angle, centered on the B candidate momentum.

In addition to the isolation variables, a method to perform an analytic reconstruction of the $B \to \tau^+\tau^-$ decay chain, described in detail in Refs. [35,36], has been developed. It combines geometrical information about the decay and mass constraints on the particles (B, τ, and ν) in the decay chain to calculate the τ momenta analytically. The possible solutions for the two τ momenta are found as solutions of a system of two coupled equations of second degree with two unknowns. The finite detector resolution and approximations made in the calculation prevent real solutions being found for a substantial fraction of the signal events. However, several intermediate quantities associated with the method are exploited to discriminate signal from background.

To make full use of the discrimination power present in the distributions of the selection variables, a requirement is

added on the output of a neural network [37], built using seven variables: the $\tau^{\pm}$ candidate masses and decay times, a charged track isolation variable for the pions, a neutral isolation variable for the B candidate, and one variable from the analytic reconstruction method, introduced in Ref. [36]. The classifier is trained on simulated $B \to \tau^+\tau^-$ decays, representing the signal, and data events from the signal-depleted region.

In order to determine the signal yield, a binned maximum likelihood fit is performed on the output of a second neural network (NN), built with 29 variables and using the same training samples. The NN inputs include the eight variables from the analytic reconstruction method listed in Ref. [36], further isolation variables, as well as kinematic and geometrical variables. The NN output is transformed to obtain a flat distribution for the signal over the range [0.0, 1.0], while the background peaks towards zero.

Varying the two-pion invariant mass sector boundaries, the signal region is optimised for the $B_s^0 \to \tau^+\tau^-$ branching fraction limit using pseudoexperiments. The boundaries are set to 615 and 935 MeV/c^2. The overall efficiency of the selection, determined using simulated $B^0_{(s)} \to \tau^+\tau^-$ decays, is approximately $2.2(2.4) \times 10^{-5}$, including the geometrical acceptance. Assuming the SM prediction, the number of $B_s^0 \to \tau^+\tau^-$ decays expected in the signal region is 0.02.

After the selection, the signal, signal-depleted, and control regions contain, respectively, 16%, 13%, and 58% of the simulated signal decays. The corresponding fractions of selected candidates in data are 7%, 37%, and 47%. Most signal decays fall into the control region, but the signal region, which contains about 14 700 candidates in data after the full selection, is more sensitive due to its lower background contamination. For the fit, ten equally sized bins of NN output in the range [0.0, 1.0] are considered, where the high NN region [0.7, 1.0] was not investigated until the fit strategy was fixed. The signal model is taken from the $B_s^0 \to \tau^+\tau^-$ simulation, while the background model is taken from the data control region, correcting for the presence of expected signal events in this region. The fit model is given by

$$\mathcal{N}^{\mathrm{SR}}_{\mathrm{data}} = s\hat{\mathcal{N}}^{\mathrm{SR}}_{\mathrm{sim}} + f_b\left(\mathcal{N}^{\mathrm{CR}}_{\mathrm{data}} - s\frac{\varepsilon^{\mathrm{CR}}}{\varepsilon^{\mathrm{SR}}}\hat{\mathcal{N}}^{\mathrm{CR}}_{\mathrm{sim}}\right), \quad (1)$$

where $\mathcal{N}^{\mathrm{SR}}_{\mathrm{sim(data)}}$ ($\mathcal{N}^{\mathrm{CR}}_{\mathrm{sim(data)}}$) is the NN output distribution in the signal (control) region from simulation (data), s is the signal yield in the signal region, f_b is a scaling factor for the background template, and $\varepsilon^{\mathrm{SR}}$ ($\varepsilon^{\mathrm{CR}}$) is the signal efficiency in the signal (control) region. The quantities s and f_b are left free in the fit. The corresponding normalized distributions $\hat{\mathcal{N}}^{\mathrm{SR}}_{\mathrm{sim}}$, $\hat{\mathcal{N}}^{\mathrm{CR}}_{\mathrm{sim}}$, and $\hat{\mathcal{N}}^{\mathrm{CR}}_{\mathrm{data}}$ are shown in Fig. 2.

The agreement between the background NN output distributions in the control and signal regions has been tested in different samples: in the data for the background-dominated NN output bins [0.0, 0.7], in a generic $b\bar{b}$ simulated sample and in several specific simulated background modes (such as $B^0 \to D^-\pi^+\pi^-\pi^+$ with $D^- \to K^0\pi^-\pi^+\pi^-$, or $B_s^0 \to D_s^-\pi^+\pi^-\pi^+$ with $D_s^- \to \tau^-\nu_\tau$). Within the statistical uncertainty, the distributions have been found to agree with each other in all cases. The background in the control region can therefore be used to characterize the background in the signal region.

Differences between the shapes of the background distribution in the signal and control regions of the data are the main sources of systematic uncertainties on the background model. These uncertainties are taken into account by allowing each bin in the $\mathcal{N}^{\mathrm{CR}}_{\mathrm{data}}$ distribution to vary according to a Gaussian constraint. The width of this Gaussian function is determined by splitting the control region into two approximately equally populated samples and taking, for each bin, the maximum difference between the NN outputs of the two subregions and the unsplit sample. The splitting is constructed to have one region more signal-like and one region more backgroundlike.

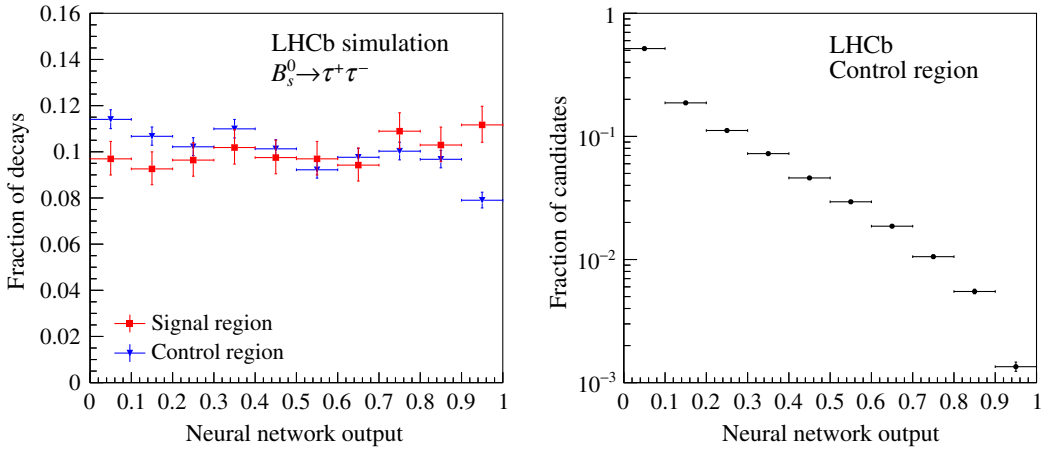

FIG. 2. (Left) Normalized NN output distribution in the signal ($\hat{\mathcal{N}}^{\mathrm{SR}}_{\mathrm{sim}}$) and control ($\hat{\mathcal{N}}^{\mathrm{CR}}_{\mathrm{sim}}$) region for $B_s^0 \to \tau^+\tau^-$ simulated events. (Right) Normalized NN output distribution in the data control region $\hat{\mathcal{N}}^{\mathrm{CR}}_{\mathrm{data}}$. The uncertainties reflect the statistics of the (simulated) data.

The signal can be mismodeled in the simulation. The $B^0 \to D^- D_s^+$ decay is used to compare data and simulation for the variables used in the NN. Ten variables are found to be slightly mismodeled and their distributions are corrected by weighting. The difference in the shape of the NN output distribution compared to the original unweighted sample is used to derive the associated systematic uncertainty. The fit procedure is validated with pseudoexperiments and is found to be unbiased. Assuming no signal contribution, the expected statistical (systematic) uncertainty on the signal yield is $^{+62}_{-40}$ ($^{+40}_{-42}$). The fit result on data is shown in Fig. 3 and gives a signal yield $s = -23^{+63}_{-53}(\text{stat})^{+41}_{-40}(\text{syst})$, where the split between the statistical and systematic uncertainties is based on the ratio expected from pseudoexperiments.

The $B_s^0 \to \tau^+\tau^-$ signal yield is converted into a branching fraction using $\mathcal{B}(B_s^0 \to \tau^+\tau^-) = \alpha^s s$, with

$$\alpha^s \equiv \frac{\epsilon^{D^-D_s^+}\mathcal{B}(B^0 \to D^- D_s^+)\mathcal{B}(D^+ \to K^-\pi^+\pi^+)\mathcal{B}(D_s^+ \to K^+K^-\pi^+)}{N^{\text{obs}}_{D^-D_s^+}\epsilon^{\tau^+\tau^-}[\mathcal{B}(\tau^- \to \pi^-\pi^+\pi^-\nu_\tau)]^2}\frac{f_d}{f_s}, \tag{2}$$

where $\epsilon^{\tau^+\tau^-}$ and $\epsilon^{D^-D_s^+}$ are the combined efficiencies of trigger, reconstruction, and selection of the signal and normalization channels. The branching fractions used are $\mathcal{B}(B^0 \to D^- D_s^+) = (7.5 \pm 1.1) \times 10^{-3}$ [19], $\mathcal{B}(D^- \to K^+\pi^-\pi^-) = (9.46 \pm 0.24)\%$ [18] and $\mathcal{B}(D_s^+ \to K^-K^+\pi^+) = (5.45 \pm 0.17)\%$ [18], and $f_s/f_d = 0.259 \pm 0.015$ [38] is the ratio of B_s^0 to B^0 production fractions. The efficiencies are determined using simulation, applying correction factors derived from data. The $B^0 \to D^- D_s^+$ yield, $N^{\text{obs}}_{D^-D_s^+}$, is obtained from a fit to the mass distribution, which has four contributions: the $B^0 \to D^- D_s^+$ component, modeled by a Hypatia function [39], a combinatorial background component, described by an exponential function, and two partially reconstructed backgrounds, $B^0 \to D^{*-} D_s^+$ and $B^0 \to D^- D_s^{*+}$, modeled as in Ref. [40]. The resulting fit is shown in Fig. 4 and gives a yield of $N^{\text{obs}}_{D^-D_s^+} = 10629 \pm 114$, where the uncertainty is statistical.

Uncertainties on α^s arise from the $B^0 \to D^- D_s^+$ fit model, the finite size of the simulated samples, the uncertainty from the corrections to the simulation and external inputs. The latter contribution, which includes the branching fractions and hadronization fractions in Eq. (2), is dominant, giving a relative uncertainty of 17% on α^s. The $B^0 \to D^- D_s^+$ fit model is varied using the sum of two Gaussian functions with a common mean and power-law tails instead of the Hypatia function for the signal, a second-order Chebyshev polynomial instead of an exponential function for the combinatorial background, and adding two other background components

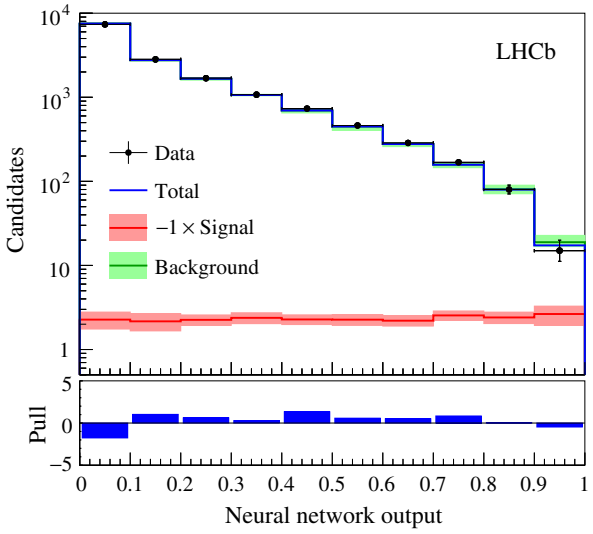

FIG. 3. Distribution of the NN output in the signal region $\mathcal{N}^{\text{SR}}_{\text{data}}$ (black points), with the total fit result (blue line) and the background component (green line). The fitted $B_s^0 \to \tau^+\tau^-$ signal component is negative and is therefore shown multiplied by −1 (red line). For each bin of the signal and background component the combined statistical and systematic uncertainty on the template is shown as a light-colored band. The difference between data and fit divided by its uncertainty (pull) is shown underneath.

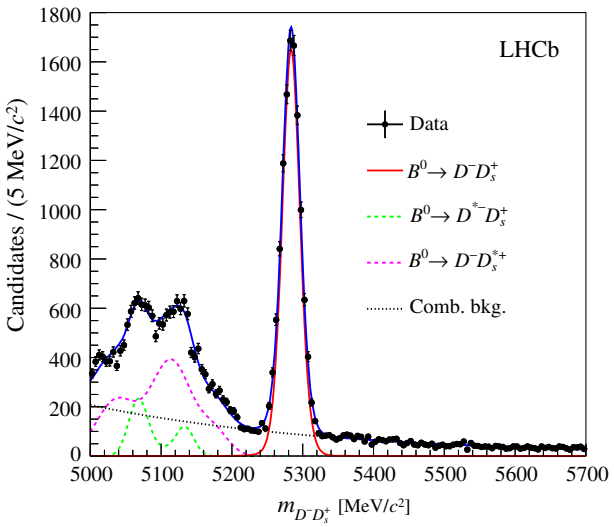

FIG. 4. Invariant mass distribution of the reconstructed $B^0 \to D^- D_s^+$ candidates in data (black points), together with the total fit result (blue line) used to determine the $B^0 \to D^- D_s^+$ yield. The individual components are described in the text.

from $B_s^0 \to D^- D_s^{*+}$ and $B^0 \to a_1(1260)^- D_s^{*+}$ decays. The change in signal yield compared to the nominal fit is taken as a systematic uncertainty, adding the contributions from the four variations in quadrature. The overall relative uncertainty on α^s due to $N^{\rm obs}_{D^- D_s^+}$ (including the fit uncertainty) is 1.7%. Corrections determined from $J/\psi \to \mu^+\mu^-$ and $D^0 \to K^-\pi^+$ data control samples are applied for the tracking, PID, and the hadronic hardware trigger efficiencies. The relative uncertainty on α^s due to selection efficiencies is 2.9%, taking into account both the limited size of the simulated samples and the systematic uncertainties. The normalization factor is found to be $\alpha^s = (4.07 \pm 0.70) \times 10^{-5}$.

The shapes of the NN output distributions and the selection efficiencies depend on the parametrization used in the simulation to model the $\tau^- \to \pi^-\pi^+\pi^-\nu_\tau$ decay. The result obtained with the TAUOLA *BABAR*-tune model is therefore compared to available alternatives [41], which are based on CLEO data for the $\tau^- \to \pi^-\pi^0\pi^0\nu_\tau$ decay [42]. The selection efficiency for these alternative models can be up to 20% higher, due to different structures in the two-pion invariant mass, resulting in lower limits. Dependence of the NN signal output distribution on the τ-decay model is found to be negligible. Since the alternative models are based on a different τ decay, the *BABAR*-tune model is chosen as default and no systematic uncertainty is assigned.

The signal yield obtained from the likelihood fit is translated into an upper limit on the $B_s^0 \to \tau^+\tau^-$ branching fraction using the CL_s method [43,44]. Assuming no contribution from $B^0 \to \tau^+\tau^-$ decays, an upper limit is set on the $B_s^0 \to \tau^+\tau^-$ branching fraction of $5.2(6.8) \times 10^{-3}$ at 90% (95%) C.L. This is the first experimental limit on $\mathcal{B}(B_s^0 \to \tau^+\tau^-)$. The analysis is repeated for the $B^0 \to \tau^+\tau^-$ decay. The fit is performed by replacing the signal model with that derived from simulated $B^0 \to \tau^+\tau^-$ decays, giving $s = -15^{+67}_{-56}(\mathrm{stat})^{+44}_{-42}(\mathrm{syst})$ [36]. The expected statistical (systematic) uncertainty on the signal yield is $^{+64}_{-58}$ ($^{+41}_{-43}$). The corresponding normalization factor is $\alpha^d = (1.16 \pm 0.19) \times 10^{-5}$. The limit obtained is $\mathcal{B}(B^0 \to \tau^+\tau^-) < 1.6(2.1) \times 10^{-3}$ at 90% (95%) C.L., which constitutes a factor of 2.6 improvement with respect to the *BABAR* result [13] and is the current best limit on $\mathcal{B}(B^0 \to \tau^+\tau^-)$.

We thank Jérôme Charles (CPT, Marseille, France) for fruitful discussions and help in developing the analytic reconstruction method. We express our gratitude to our colleagues in the CERN accelerator departments for the excellent performance of the LHC. We thank the technical and administrative staff at the LHCb institutes. We acknowledge support from CERN and from the national agencies: CAPES, CNPq, FAPERJ, and FINEP (Brazil); MOST and NSFC (China); CNRS/IN2P3 (France); BMBF, DFG, and MPG (Germany); INFN (Italy); FOM and NWO (Netherlands); MNiSW and NCN (Poland); MEN/IFA (Romania); MinES and FASO (Russia); MinECo (Spain); SNSF and SER (Switzerland); NASU (Ukraine); STFC (United Kingdom); and NSF (USA). We acknowledge the computing resources that are provided by CERN, IN2P3 (France), KIT and DESY (Germany), INFN (Italy), SURF (Netherlands), PIC (Spain), GridPP (United Kingdom), RRCKI and Yandex LLC (Russia), CSCS (Switzerland), IFIN-HH (Romania), CBPF (Brazil), PL-GRID (Poland), and OSC (USA). We are indebted to the communities behind the multiple open source software packages on which we depend. Individual groups or members have received support from AvH Foundation (Germany), EPLANET, Marie Skłodowska-Curie Actions and ERC (European Union), Conseil Général de Haute-Savoie, Labex ENIGMASS, and OCEVU, Région Auvergne (France), RFBR and Yandex LLC (Russia), GVA, XuntaGal, and GENCAT (Spain), Herchel Smith Fund, The Royal Society, Royal Commission for the Exhibition of 1851, and the Leverhulme Trust (United Kingdom).

[1] V. Khachatryan *et al.* (CMS and LHCb Collaborations), Observation of the rare $B_s^0 \to \mu^+\mu^-$ decay from the combined analysis of CMS and LHCb data, Nature (London) **522**, 68 (2015).

[2] R. Aaij *et al.* (LHCb Collaboration), Measurement of the $B_s^0 \to \mu^+\mu^-$ branching fraction and effective lifetime and search for $B^0 \to \mu^+\mu^-$ decays, Phys. Rev. Lett. **118**, 191801 (2017).

[3] C. Bobeth, M. Gorbahn, T. Hermann, M. Misiak, E. Stamou, and M. Steinhauser, $B_{s,d} \to \ell^+\ell^-$ in the Standard Model with Reduced Theoretical Uncertainty, Phys. Rev. Lett. **112**, 101801 (2014).

[4] Y. Amhis *et al.* (Heavy Flavor Averaging Group Collaboration), Averages of b-hadron, c-hadron, and τ-lepton properties as of summer 2016, arXiv:1612.07233, http://www.slac.stanford.edu/xorg/hfag/.

[5] R. Aaij *et al.* (LHCb Collaboration), Test of Lepton Universality Using $B^+ \to K^+\ell\ell$ Decays, Phys. Rev. Lett. **113**, 151601 (2014).

[6] R. Aaij *et al.* (LHCb Collaboration), Angular analysis of the $B^0 \to K^{*0}\mu^+\mu^-$ decay using 3 fb^{-1} of integrated luminosity, J. High Energy Phys. 02 (2016) 104.

[7] A. Crivellin, G. D'Ambrosio, and J. Heeck, Addressing the LHC flavor anomalies with horizontal gauge symmetries, Phys. Rev. D **91**, 075006 (2015).

[8] D. Bečirević, S. Fajfer, N. Košnik, and O. Sumensari, Leptoquark model to explain the B-physics anomalies, R_K and R_D, Phys. Rev. D **94**, 115021 (2016).

[9] A. Dighe and D. Ghosh, How large can the branching ratio of $B_s^0 \to \tau^+\tau^-$ be?, Phys. Rev. D **86**, 054023 (2012).

[10] R. Alonso, B. Grinstein, and J. M. Camalich, Lepton universality violation and lepton flavor conservation in B-meson decays, J. High Energy Phys. 10 (2015) 184.

[11] J. M. Cline, Scalar doublet models confront τ and b anomalies, Phys. Rev. D **93**, 075017 (2016).

[12] D. Bečirević, N. Košnik, O. Sumensari, and R. Z. Funchal, Palatable leptoquark scenarios for lepton flavor violation in exclusive $b \to s\ell_1\ell_2$ modes, J. High Energy Phys. 11 (2016) 035.

[13] B. Aubert *et al.* (*BABAR* Collaboration), A Search for the Rare Decay $B^0 \to \tau^+\tau^-$ at *BABAR*, Phys. Rev. Lett. **96**, 241802 (2006).

[14] Y. Grossman, Z. Ligeti, and E. Nardi, $B \to \tau^+\tau^-(X)$ decays: First constraints and phenomenological implications, Phys. Rev. D **55**, 2768 (1997).

[15] A. Dighe, A. Kundu, and S. Nandi, Enhanced $B_s^0 - \bar{B}_s^0$ lifetime difference and anomalous like-sign dimuon charge asymmetry from new physics in $B_s^0 \to \tau^+\tau^-$, Phys. Rev. D **82**, 031502 (2010).

[16] C. Bobeth and U. Haisch, New physics in Γ_{12}^s: $(\bar{s}b)(\bar{\tau}\tau)$ operators, Acta Phys. Pol. B **44**, 127 (2013).

[17] S. Schael *et al.* (ALEPH Collaboration), Branching ratios and spectral functions of tau decays: Final ALEPH measurements and physics implications, Phys. Rep. **421**, 191 (2005).

[18] C. Patrignani *et al.* (Particle Data Group Collabortion), Review of particle physics, Chin. Phys. C **40**, 100001 (2016).

[19] A. Zupanc *et al.* (Belle Collaboration), Improved measurement of $\bar{B}^0 \to D_s^- D^+$ and search for $\bar{B}^0 \to D_s^+ D_s^-$ at Belle, Phys. Rev. D **75**, 091102 (2007).

[20] B. Aubert *et al.* (*BABAR* Collaboration), Study of $B \to D^{(*)} D_{s(J)}^{(*)}$ decays and measurement of D_s^- and $D_{sJ}(2460)^-$ branching fractions, Phys. Rev. D **74**, 031103 (2006).

[21] A. A. Alves Jr. *et al.* (LHCb Collaboration), The LHCb detector at the LHC, J. Instrum. **3**, S08005 (2008).

[22] R. Aaij *et al.* (LHCb Collaboration), LHCb detector performance, Int. J. Mod. Phys. A **30**, 1530022 (2015).

[23] R. Aaij *et al.*, The LHCb trigger and its performance in 2011, J. Instrum. **8**, P04022 (2013).

[24] V. V. Gligorov and M. Williams, Efficient, reliable and fast high-level triggering using a bonsai boosted decision tree, J. Instrum. **8**, P02013 (2013).

[25] T. Sjöstrand, S. Mrenna, and P. Skands, PYTHIA 6.4 physics and manual, J. High Energy Phys. 05 (2006) 026; A brief introduction to PYTHIA 8.1, Comput. Phys. Commun. **178**, 852 (2008).

[26] I. Belyaev *et al.*, Handling of the generation of primary events in Gauss, the LHCb simulation framework, J. Phys. Conf. Ser. **331**, 032047 (2011).

[27] D. J. Lange, The EvtGen particle decay simulation package, Nucl. Instrum. Methods Phys. Res., Sect. A **462**, 152 (2001).

[28] P. Golonka and Z. Was, PHOTOS Monte Carlo: A precision tool for QED corrections in Z and W decays, Eur. Phys. J. C **45**, 97 (2006).

[29] J. Allison *et al.* (Geant4 Collaboration), Geant4 developments and applications, IEEE Trans. Nucl. Sci. **53**, 270 (2006); S. Agostinelli *et al.* (Geant4 Collaboration), Geant4: A simulation toolkit, Nucl. Instrum. Methods Phys. Res., Sect. A **506**, 250 (2003).

[30] M. Clemencic, G. Corti, S. Easo, C. R Jones, S. Miglioranzi, M. Pappagallo, and P. Robbe, The LHCb simulation application, Gauss: Design, evolution and experience, J. Phys. Conf. Ser. **331**, 032023 (2011).

[31] I. M. Nugent, T. Przedzinski, P. Roig, O. Shekhovtsova, and Z. Was, Resonance chiral Lagrangian currents and experimental data for $\tau^- \to \pi^-\pi^-\pi^+\nu_\tau$, Phys. Rev. D **88**, 093012 (2013).

[32] I. M. Nugent, Invariant mass spectra of $\tau^- \to h^-h^-h^+\nu_\tau$ decays, Nucl. Phys. B, Proc. Suppl. **253–255**, 38 (2014).

[33] N. Davidson, G. Nanava, T. Przedziński, E. Richter-Wąs, and Z. Wąs, Universal interface of TAUOLA technical and physics documentation, Comput. Phys. Commun. **183**, 821 (2012).

[34] M. Adinolfi *et al.*, Performance of the LHCb RICH detector at the LHC, Eur. Phys. J. C **73**, 2431 (2013).

[35] A. Mordà, Ph.D. thesis, Aix-Marseille Université, [CERN Report No. CERN-THESIS-2015-264, 2015 (unpublished)].

[36] See Supplemental Material at http://link.aps.org/supplemental/10.1103/PhysRevLett.118.251802 for further details.

[37] M. Feindt, A neural Bayesian estimator for conditional probability densities, arXiv:physics/0402093.

[38] R. Aaij *et al.* (LHCb Collaboration), Measurement of the fragmentation fraction ratio f_s/f_d and its dependence on B meson kinematics, J. High Energy Phys. 04 (2013) 001, f_s/f_d value updated in Report No. LHCb-CONF-2013-011.

[39] D. M. Santos and F. Dupertuis, Mass distributions marginalized over per-event errors, Nucl. Instrum. Methods Phys. Res., Sect. A **764**, 150 (2014).

[40] R. Aaij *et al.* (LHCb Collaboration), First observations of $\bar{B}_s^0 \to D^+D^-$, $D_s^+D^-$ and $D^0\bar{D}^0$ decays, Phys. Rev. D **87**, 092007 (2013).

[41] Z. Was and J. Zaremba, Study of variants for Monte Carlo generators of $\tau \to 3\pi\nu$ decays, Eur. Phys. J. C **75**, 566 (2015).

[42] D. M. Asner *et al.* (CLEO Collaboration), Hadronic structure in the decay $\tau^- \to \nu_\tau\pi^-\pi^0\pi^0$ and the sign of the tau neutrino helicity, Phys. Rev. D **61**, 012002 (1999).

[43] A. L. Read, Presentation of search results: The CL_s technique, J. Phys. G **28**, 2693 (2002).

[44] G. Cowan, K. Cranmer, E. Gross, and O. Vitells, Asymptotic formulae for likelihood-based tests of new physics, Eur. Phys. J. C **71**, 1554 (2011); Erratum, Eur. Phys. J. C **73**, 2501(E) (2013).

R. Aaij,[40] B. Adeva,[39] M. Adinolfi,[48] Z. Ajaltouni,[5] S. Akar,[59] J. Albrecht,[10] F. Alessio,[40] M. Alexander,[53] S. Ali,[43] G. Alkhazov,[31] P. Alvarez Cartelle,[55] A. A. Alves Jr.,[59] S. Amato,[2] S. Amerio,[23] Y. Amhis,[7] L. An,[3] L. Anderlini,[18] G. Andreassi,[41] M. Andreotti,[17,a] J. E. Andrews,[60] R. B. Appleby,[56] F. Archilli,[43] P. d'Argent,[12] J. Arnau Romeu,[6] A. Artamonov,[37] M. Artuso,[61] E. Aslanides,[6] G. Auriemma,[26] M. Baalouch,[5] I. Babuschkin,[56] S. Bachmann,[12] J. J. Back,[50] A. Badalov,[38] C. Baesso,[62] S. Baker,[55] V. Balagura,[7,b] W. Baldini,[17] A. Baranov,[35] R. J. Barlow,[56] C. Barschel,[40] S. Barsuk,[7]

W. Barter,[56] F. Baryshnikov,[32] M. Baszczyk,[27] V. Batozskaya,[29] B. Batsukh,[61] V. Battista,[41] A. Bay,[41] L. Beaucourt,[4] J. Beddow,[53] F. Bedeschi,[24] I. Bediaga,[1] A. Beiter,[61] L. J. Bel,[43] V. Bellee,[41] N. Belloli,[21,c] K. Belous,[37] I. Belyaev,[32] E. Ben-Haim,[8] G. Bencivenni,[19] S. Benson,[43] S. Beranek,[9] A. Berezhnoy,[33] R. Bernet,[42] A. Bertolin,[23] C. Betancourt,[42] F. Betti,[15] M.-O. Bettler,[40] M. van Beuzekom,[43] Ia. Bezshyiko,[42] S. Bifani,[47] P. Billoir,[8] A. Birnkraut,[10] A. Bitadze,[56] A. Bizzeti,[18,d] T. Blake,[50] F. Blanc,[41] J. Blouw,[11] S. Blusk,[61] V. Bocci,[26] T. Boettcher,[58] A. Bondar,[36,e] N. Bondar,[31] W. Bonivento,[16] I. Bordyuzhin,[32] A. Borgheresi,[21,c] S. Borghi,[56] M. Borisyak,[35] M. Borsato,[39] F. Bossu,[7] M. Boubdir,[9] T. J. V. Bowcock,[54] E. Bowen,[42] C. Bozzi,[17,40] S. Braun,[12] T. Britton,[61] J. Brodzicka,[56] E. Buchanan,[48] C. Burr,[56] A. Bursche,[2] J. Buytaert,[40] S. Cadeddu,[16] R. Calabrese,[17,a] M. Calvi,[21,c] M. Calvo Gomez,[38,f] A. Camboni,[38] P. Campana,[19] D. H. Campora Perez,[40] L. Capriotti,[56] A. Carbone,[15,g] G. Carboni,[25,h] R. Cardinale,[20,i] A. Cardini,[16] P. Carniti,[21,c] L. Carson,[52] K. Carvalho Akiba,[2] G. Casse,[54] L. Cassina,[21,c] L. Castillo Garcia,[41] M. Cattaneo,[40] G. Cavallero,[20] R. Cenci,[24,j] D. Chamont,[7] M. Charles,[8] Ph. Charpentier,[40] G. Chatzikonstantinidis,[47] M. Chefdeville,[4] S. Chen,[56] S.-F. Cheung,[57] V. Chobanova,[39] M. Chrzaszcz,[42,27] A. Chubykin,[31] X. Cid Vidal,[39] G. Ciezarek,[43] P. E. L. Clarke,[52] M. Clemencic,[40] H. V. Cliff,[49] J. Closier,[40] V. Coco,[59] J. Cogan,[6] E. Cogneras,[5] V. Cogoni,[16,k] L. Cojocariu,[30] P. Collins,[40] A. Comerma-Montells,[12] A. Contu,[40] A. Cook,[48] G. Coombs,[40] S. Coquereau,[38] G. Corti,[40] M. Corvo,[17,a] C. M. Costa Sobral,[50] B. Couturier,[40] G. A. Cowan,[52] D. C. Craik,[52] A. Crocombe,[50] M. Cruz Torres,[62] S. Cunliffe,[55] R. Currie,[52] C. D'Ambrosio,[40] F. Da Cunha Marinho,[2] E. Dall'Occo,[43] J. Dalseno,[48] P. N. Y. David,[43] A. Davis,[3] K. De Bruyn,[6] S. De Capua,[56] M. De Cian,[12] J. M. De Miranda,[1] L. De Paula,[2] M. De Serio,[14,l] P. De Simone,[19] C. T. Dean,[53] D. Decamp,[4] M. Deckenhoff,[10] L. Del Buono,[8] H.-P. Dembinski,[11] M. Demmer,[10] A. Dendek,[28] D. Derkach,[35] O. Deschamps,[5] F. Dettori,[54] B. Dey,[22] A. Di Canto,[40] P. Di Nezza,[19] H. Dijkstra,[40] F. Dordei,[40] M. Dorigo,[41] A. Dosil Suárez,[39] A. Dovbnya,[45] K. Dreimanis,[54] L. Dufour,[43] G. Dujany,[56] K. Dungs,[40] P. Durante,[40] R. Dzhelyadin,[37] M. Dziewiecki,[12] A. Dziurda,[40] A. Dzyuba,[31] N. Déléage,[4] S. Easo,[51] M. Ebert,[52] U. Egede,[55] V. Egorychev,[32] S. Eidelman,[36,e] S. Eisenhardt,[52] U. Eitschberger,[10] R. Ekelhof,[10] L. Eklund,[53] S. Ely,[61] S. Esen,[12] H. M. Evans,[49] T. Evans,[57] A. Falabella,[15] N. Farley,[47] S. Farry,[54] R. Fay,[54] D. Fazzini,[21,c] D. Ferguson,[52] G. Fernandez,[38] A. Fernandez Prieto,[39] F. Ferrari,[15] F. Ferreira Rodrigues,[2] M. Ferro-Luzzi,[40] S. Filippov,[34] R. A. Fini,[14] M. Fiore,[17,a] M. Fiorini,[17,a] M. Firlej,[28] C. Fitzpatrick,[41] T. Fiutowski,[28] F. Fleuret,[7,m] K. Fohl,[40] M. Fontana,[16,40] F. Fontanelli,[20,i] D. C. Forshaw,[61] R. Forty,[40] V. Franco Lima,[54] M. Frank,[40] C. Frei,[40] J. Fu,[22,n] W. Funk,[40] E. Furfaro,[25,h] C. Färber,[40] A. Gallas Torreira,[39] D. Galli,[15,g] S. Gallorini,[23] S. Gambetta,[52] M. Gandelman,[2] P. Gandini,[57] Y. Gao,[3] L. M. Garcia Martin,[69] J. García Pardiñas,[39] J. Garra Tico,[49] L. Garrido,[38] P. J. Garsed,[49] D. Gascon,[38] C. Gaspar,[40] L. Gavardi,[10] G. Gazzoni,[5] D. Gerick,[12] E. Gersabeck,[12] M. Gersabeck,[56] T. Gershon,[50] Ph. Ghez,[4] S. Gianì,[41] V. Gibson,[49] O. G. Girard,[41] L. Giubega,[30] K. Gizdov,[52] V. V. Gligorov,[8] D. Golubkov,[32] A. Golutvin,[55,40] A. Gomes,[1,o] I. V. Gorelov,[33] C. Gotti,[21,c] E. Govorkova,[43] R. Graciani Diaz,[38] L. A. Granado Cardoso,[40] E. Graugés,[38] E. Graverini,[42] G. Graziani,[18] A. Grecu,[30] R. Greim,[9] P. Griffith,[16] L. Grillo,[21,40,c] B. R. Gruberg Cazon,[57] O. Grünberg,[67] E. Gushchin,[34] Yu. Guz,[37] T. Gys,[40] C. Göbel,[62] T. Hadavizadeh,[57] C. Hadjivasiliou,[5] G. Haefeli,[41] C. Haen,[40] S. C. Haines,[49] B. Hamilton,[60] X. Han,[12] S. Hansmann-Menzemer,[12] N. Harnew,[57] S. T. Harnew,[48] J. Harrison,[56] M. Hatch,[40] J. He,[63] T. Head,[41] A. Heister,[9] K. Hennessy,[54] P. Henrard,[5] L. Henry,[69] E. van Herwijnen,[40] M. Heß,[67] A. Hicheur,[2] D. Hill,[57] C. Hombach,[56] H. Hopchev,[41] Z.-C. Huard,[59] W. Hulsbergen,[43] T. Humair,[55] M. Hushchyn,[35] D. Hutchcroft,[54] M. Idzik,[28] P. Ilten,[58] R. Jacobsson,[40] J. Jalocha,[57] E. Jans,[43] A. Jawahery,[60] F. Jiang,[3] M. John,[57] D. Johnson,[40] C. R. Jones,[49] C. Joram,[40] B. Jost,[40] N. Jurik,[57] S. Kandybei,[45] M. Karacson,[40] J. M. Kariuki,[48] S. Karodia,[53] M. Kecke,[12] M. Kelsey,[61] M. Kenzie,[49] T. Ketel,[44] E. Khairullin,[35] B. Khanji,[12] C. Khurewathanakul,[41] T. Kirn,[9] S. Klaver,[56] K. Klimaszewski,[29] T. Klimkovich,[11] S. Koliiev,[46] M. Kolpin,[12] I. Komarov,[41] R. Kopecna,[12] P. Koppenburg,[43] A. Kosmyntseva,[32] S. Kotriakhova,[31] A. Kozachuk,[33] M. Kozeiha,[5] L. Kravchuk,[34] M. Kreps,[50] P. Krokovny,[36,e] F. Kruse,[10] W. Krzemien,[29] W. Kucewicz,[27,p] M. Kucharczyk,[27] V. Kudryavtsev,[36,e] A. K. Kuonen,[41] K. Kurek,[29] T. Kvaratskheliya,[32,40] D. Lacarrere,[40] G. Lafferty,[56] A. Lai,[16] G. Lanfranchi,[19] C. Langenbruch,[9] T. Latham,[50] C. Lazzeroni,[47] R. Le Gac,[6] J. van Leerdam,[43] A. Leflat,[33,40] J. Lefrançois,[7] R. Lefèvre,[5] F. Lemaitre,[40] E. Lemos Cid,[39] O. Leroy,[6] T. Lesiak,[27] B. Leverington,[12] T. Li,[3] Y. Li,[7] Z. Li,[61] T. Likhomanenko,[35,68] R. Lindner,[40] F. Lionetto,[42] X. Liu,[3] D. Loh,[50] I. Longstaff,[53] J. H. Lopes,[2] D. Lucchesi,[23,q] M. Lucio Martinez,[39] H. Luo,[52] A. Lupato,[23] E. Luppi,[17,a] O. Lupton,[40] A. Lusiani,[24] X. Lyu,[63] F. Machefert,[7] F. Maciuc,[30] O. Maev,[31] K. Maguire,[56] S. Malde,[57] A. Malinin,[68] T. Maltsev,[36] G. Manca,[16,k] G. Mancinelli,[6] P. Manning,[61] J. Maratas,[5,r] J. F. Marchand,[4] U. Marconi,[15] C. Marin Benito,[38] M. Marinangeli,[41] P. Marino,[24,j] J. Marks,[12] G. Martellotti,[26] M. Martin,[6] M. Martinelli,[41] D. Martinez Santos,[39] F. Martinez Vidal,[69] D. Martins Tostes,[2] L. M. Massacrier,[7] A. Massafferri,[1]

R. Matev,[40] A. Mathad,[50] Z. Mathe,[40] C. Matteuzzi,[21] A. Mauri,[42] E. Maurice,[7,m] B. Maurin,[41] A. Mazurov,[47] M. McCann,[55,40] A. McNab,[56] R. McNulty,[13] B. Meadows,[59] F. Meier,[10] D. Melnychuk,[29] M. Merk,[43] A. Merli,[22,n] E. Michielin,[23] D. A. Milanes,[66] M.-N. Minard,[4] D. S. Mitzel,[12] A. Mogini,[8] J. Molina Rodriguez,[1] I. A. Monroy,[66] S. Monteil,[5] M. Morandin,[23] A. Mordà,[6] M. J. Morello,[24,j] O. Morgunova,[68] J. Moron,[28] A. B. Morris,[52] R. Mountain,[61] F. Muheim,[52] M. Mulder,[43] M. Mussini,[15] D. Müller,[56] J. Müller,[10] K. Müller,[42] V. Müller,[10] P. Naik,[48] T. Nakada,[41] R. Nandakumar,[51] A. Nandi,[57] I. Nasteva,[2] M. Needham,[52] N. Neri,[22,40] S. Neubert,[12] N. Neufeld,[40] M. Neuner,[12] T. D. Nguyen,[41] C. Nguyen-Mau,[41,s] S. Nieswand,[9] R. Niet,[10] N. Nikitin,[33] T. Nikodem,[12] A. Nogay,[68] A. Novoselov,[37] D. P. O'Hanlon,[50] A. Oblakowska-Mucha,[28] V. Obraztsov,[37] S. Ogilvy,[19] R. Oldeman,[16,k] C. J. G. Onderwater,[70] A. Ossowska,[27] J. M. Otalora Goicochea,[2] P. Owen,[42] A. Oyanguren,[69] P. R. Pais,[41] A. Palano,[14,l] M. Palutan,[19,40] A. Papanestis,[51] M. Pappagallo,[14,l] L. L. Pappalardo,[17,a] C. Pappenheimer,[59] W. Parker,[60] C. Parkes,[56] G. Passaleva,[18] A. Pastore,[14,l] M. Patel,[55] C. Patrignani,[15,g] A. Pearce,[40] A. Pellegrino,[43] G. Penso,[26] M. Pepe Altarelli,[40] S. Perazzini,[40] P. Perret,[5] L. Pescatore,[41] K. Petridis,[48] A. Petrolini,[20,i] A. Petrov,[68] M. Petruzzo,[22,n] E. Picatoste Olloqui,[38] B. Pietrzyk,[4] M. Pikies,[27] D. Pinci,[26] A. Pistone,[20] A. Piucci,[12] V. Placinta,[30] S. Playfer,[52] M. Plo Casasus,[39] T. Poikela,[40] F. Polci,[8] M Poli Lener,[19] A. Poluektov,[50,36] I. Polyakov,[61] E. Polycarpo,[2] G. J. Pomery,[48] S. Ponce,[40] A. Popov,[37] D. Popov,[11,40] B. Popovici,[30] S. Poslavskii,[37] C. Potterat,[2] E. Price,[48] J. Prisciandaro,[39] C. Prouve,[48] V. Pugatch,[46] A. Puig Navarro,[42] G. Punzi,[24,t] C. Qian,[63] W. Qian,[50] R. Quagliani,[7,48] B. Rachwal,[28] J. H. Rademacker,[48] M. Rama,[24] M. Ramos Pernas,[39] M. S. Rangel,[2] I. Raniuk,[45] F. Ratnikov,[35] G. Raven,[44] F. Redi,[55] S. Reichert,[10] A. C. dos Reis,[1] C. Remon Alepuz,[69] V. Renaudin,[7] S. Ricciardi,[51] S. Richards,[48] M. Rihl,[40] K. Rinnert,[54] V. Rives Molina,[38] P. Robbe,[7] A. B. Rodrigues,[1] E. Rodrigues,[59] J. A. Rodriguez Lopez,[66] P. Rodriguez Perez,[56] A. Rogozhnikov,[35] S. Roiser,[40] A. Rollings,[57] V. Romanovskiy,[37] A. Romero Vidal,[39] J. W. Ronayne,[13] M. Rotondo,[19] M. S. Rudolph,[61] T. Ruf,[40] P. Ruiz Valls,[69] J. J. Saborido Silva,[39] E. Sadykhov,[32] N. Sagidova,[31] B. Saitta,[16,k] V. Salustino Guimaraes,[1] D. Sanchez Gonzalo,[38] C. Sanchez Mayordomo,[69] B. Sanmartin Sedes,[39] R. Santacesaria,[26] C. Santamarina Rios,[39] M. Santimaria,[19] E. Santovetti,[25,h] A. Sarti,[19,u] C. Satriano,[26,v] A. Satta,[25] D. M. Saunders,[48] D. Savrina,[32,33] S. Schael,[9] M. Schellenberg,[10] M. Schiller,[53] H. Schindler,[40] M. Schlupp,[10] M. Schmelling,[11] T. Schmelzer,[10] B. Schmidt,[40] O. Schneider,[41] A. Schopper,[40] H. F. Schreiner,[59] K. Schubert,[10] M. Schubiger,[41] M.-H. Schune,[7] R. Schwemmer,[40] B. Sciascia,[19] A. Sciubba,[26,u] A. Semennikov,[32] A. Sergi,[47] N. Serra,[42] J. Serrano,[6] L. Sestini,[23] P. Seyfert,[21] M. Shapkin,[37] I. Shapoval,[45] Y. Shcheglov,[31] T. Shears,[54] L. Shekhtman,[36,e] V. Shevchenko,[68] B. G. Siddi,[17,40] R. Silva Coutinho,[42] L. Silva de Oliveira,[2] G. Simi,[23,q] S. Simone,[14,l] M. Sirendi,[49] N. Skidmore,[48] T. Skwarnicki,[61] E. Smith,[55] I. T. Smith,[52] J. Smith,[49] M. Smith,[55] l. Soares Lavra,[1] M. D. Sokoloff,[59] F. J. P. Soler,[53] B. Souza De Paula,[2] B. Spaan,[10] P. Spradlin,[53] S. Sridharan,[40] F. Stagni,[40] M. Stahl,[12] S. Stahl,[40] P. Stefko,[41] S. Stefkova,[55] O. Steinkamp,[42] S. Stemmle,[12] O. Stenyakin,[37] H. Stevens,[10] S. Stoica,[30] S. Stone,[61] B. Storaci,[42] S. Stracka,[24,t] M. E. Stramaglia,[41] M. Straticiuc,[30] U. Straumann,[42] L. Sun,[64] W. Sutcliffe,[55] K. Swientek,[28] V. Syropoulos,[44] M. Szczekowski,[29] T. Szumlak,[28] S. T'Jampens,[4] A. Tayduganov,[6] T. Tekampe,[10] G. Tellarini,[17,a] F. Teubert,[40] E. Thomas,[40] J. van Tilburg,[43] M. J. Tilley,[55] V. Tisserand,[4] M. Tobin,[41] S. Tolk,[49] L. Tomassetti,[17,a] D. Tonelli,[24] S. Topp-Joergensen,[57] F. Toriello,[61] R. Tourinho Jadallah Aoude,[1] E. Tournefier,[4] S. Tourneur,[41] K. Trabelsi,[41] M. Traill,[53] M. T. Tran,[41] M. Tresch,[42] A. Trisovic,[40] A. Tsaregorodtsev,[6] P. Tsopelas,[43] A. Tully,[49] N. Tuning,[43] A. Ukleja,[29] A. Ustyuzhanin,[35] U. Uwer,[12] C. Vacca,[16,k] V. Vagnoni,[15,40] A. Valassi,[40] S. Valat,[40] G. Valenti,[15] R. Vazquez Gomez,[19] P. Vazquez Regueiro,[39] S. Vecchi,[17] M. van Veghel,[43] J. J. Velthuis,[48] M. Veltri,[18,w] G. Veneziano,[57] A. Venkateswaran,[61] T. A. Verlage,[9] M. Vernet,[5] M. Vesterinen,[12] J. V. Viana Barbosa,[40] B. Viaud,[7] D. Vieira,[63] M. Vieites Diaz,[39] H. Viemann,[67] X. Vilasis-Cardona,[38,f] M. Vitti,[49] V. Volkov,[33] A. Vollhardt,[42] B. Voneki,[40] A. Vorobyev,[31] V. Vorobyev,[36,e] C. Voß,[9] J. A. de Vries,[43] C. Vázquez Sierra,[39] R. Waldi,[67] C. Wallace,[50] R. Wallace,[13] J. Walsh,[24] J. Wang,[61] D. R. Ward,[49] H. M. Wark,[54] N. K. Watson,[47] D. Websdale,[55] A. Weiden,[42] M. Whitehead,[40] J. Wicht,[50] G. Wilkinson,[57,40] M. Wilkinson,[61] M. Williams,[40] M. P. Williams,[47] M. Williams,[58] T. Williams,[47] F. F. Wilson,[51] J. Wimberley,[60] M. A. Winn,[7] J. Wishahi,[10] W. Wislicki,[29] M. Witek,[27] G. Wormser,[7] S. A. Wotton,[49] K. Wraight,[53] K. Wyllie,[40] Y. Xie,[65] Z. Xing,[61] Z. Xu,[4] Z. Yang,[3] Z Yang,[60] Y. Yao,[61] H. Yin,[65] J. Yu,[65] X. Yuan,[36,e] O. Yushchenko,[37] K. A. Zarebski,[47] M. Zavertyaev,[11,b] L. Zhang,[3] Y. Zhang,[7] A. Zhelezov,[12] Y. Zheng,[63] X. Zhu,[3] V. Zhukov,[33] and S. Zucchelli[15]

(LHCb Collaboration)

[1]Centro Brasileiro de Pesquisas Físicas (CBPF), Rio de Janeiro, Brazil
[2]Universidade Federal do Rio de Janeiro (UFRJ), Rio de Janeiro, Brazil
[3]Center for High Energy Physics, Tsinghua University, Beijing, China
[4]LAPP, Université Savoie Mont-Blanc, CNRS/IN2P3, Annecy-Le-Vieux, France
[5]Clermont Université, Université Blaise Pascal, CNRS/IN2P3, LPC, Clermont-Ferrand, France
[6]CPPM, Aix-Marseille Université, CNRS/IN2P3, Marseille, France
[7]LAL, Université Paris-Sud, CNRS/IN2P3, Orsay, France
[8]LPNHE, Université Pierre et Marie Curie, Université Paris Diderot, CNRS/IN2P3, Paris, France
[9]I. Physikalisches Institut, RWTH Aachen University, Aachen, Germany
[10]Fakultät Physik, Technische Universität Dortmund, Dortmund, Germany
[11]Max-Planck-Institut für Kernphysik (MPIK), Heidelberg, Germany
[12]Physikalisches Institut, Ruprecht-Karls-Universität Heidelberg, Heidelberg, Germany
[13]School of Physics, University College Dublin, Dublin, Ireland
[14]Sezione INFN di Bari, Bari, Italy
[15]Sezione INFN di Bologna, Bologna, Italy
[16]Sezione INFN di Cagliari, Cagliari, Italy
[17]Sezione INFN di Ferrara, Ferrara, Italy
[18]Sezione INFN di Firenze, Firenze, Italy
[19]Laboratori Nazionali dell'INFN di Frascati, Frascati, Italy
[20]Sezione INFN di Genova, Genova, Italy
[21]Sezione INFN di Milano Bicocca, Milano, Italy
[22]Sezione INFN di Milano, Milano, Italy
[23]Sezione INFN di Padova, Padova, Italy
[24]Sezione INFN di Pisa, Pisa, Italy
[25]Sezione INFN di Roma Tor Vergata, Roma, Italy
[26]Sezione INFN di Roma La Sapienza, Roma, Italy
[27]Henryk Niewodniczanski Institute of Nuclear Physics Polish Academy of Sciences, Kraków, Poland
[28]AGH - University of Science and Technology, Faculty of Physics and Applied Computer Science, Kraków, Poland
[29]National Center for Nuclear Research (NCBJ), Warsaw, Poland
[30]Horia Hulubei National Institute of Physics and Nuclear Engineering, Bucharest-Magurele, Romania
[31]Petersburg Nuclear Physics Institute (PNPI), Gatchina, Russia
[32]Institute of Theoretical and Experimental Physics (ITEP), Moscow, Russia
[33]Institute of Nuclear Physics, Moscow State University (SINP MSU), Moscow, Russia
[34]Institute for Nuclear Research of the Russian Academy of Sciences (INR RAN), Moscow, Russia
[35]Yandex School of Data Analysis, Moscow, Russia
[36]Budker Institute of Nuclear Physics (SB RAS), Novosibirsk, Russia
[37]Institute for High Energy Physics (IHEP), Protvino, Russia
[38]ICCUB, Universitat de Barcelona, Barcelona, Spain
[39]Universidad de Santiago de Compostela, Santiago de Compostela, Spain
[40]European Organization for Nuclear Research (CERN), Geneva, Switzerland
[41]Institute of Physics, Ecole Polytechnique Fédérale de Lausanne (EPFL), Lausanne, Switzerland
[42]Physik-Institut, Universität Zürich, Zürich, Switzerland
[43]Nikhef National Institute for Subatomic Physics, Amsterdam, Netherlands
[44]Nikhef National Institute for Subatomic Physics and VU University Amsterdam, Amsterdam, Netherlands
[45]NSC Kharkiv Institute of Physics and Technology (NSC KIPT), Kharkiv, Ukraine
[46]Institute for Nuclear Research of the National Academy of Sciences (KINR), Kyiv, Ukraine
[47]University of Birmingham, Birmingham, United Kingdom
[48]H.H. Wills Physics Laboratory, University of Bristol, Bristol, United Kingdom
[49]Cavendish Laboratory, University of Cambridge, Cambridge, United Kingdom
[50]Department of Physics, University of Warwick, Coventry, United Kingdom
[51]STFC Rutherford Appleton Laboratory, Didcot, United Kingdom
[52]School of Physics and Astronomy, University of Edinburgh, Edinburgh, United Kingdom
[53]School of Physics and Astronomy, University of Glasgow, Glasgow, United Kingdom
[54]Oliver Lodge Laboratory, University of Liverpool, Liverpool, United Kingdom
[55]Imperial College London, London, United Kingdom
[56]School of Physics and Astronomy, University of Manchester, Manchester, United Kingdom
[57]Department of Physics, University of Oxford, Oxford, United Kingdom
[58]Massachusetts Institute of Technology, Cambridge, Massachusetts, USA
[59]University of Cincinnati, Cincinnati, Ohio, USA

[60]University of Maryland, College Park, Maryland, USA
[61]Syracuse University, Syracuse, New York, USA
[62]Pontifícia Universidade Católica do Rio de Janeiro (PUC-Rio), Rio de Janeiro, Brazil
(associated with Institution Universidade Federal do Rio de Janeiro (UFRJ), Rio de Janeiro, Brazil)
[63]University of Chinese Academy of Sciences, Beijing, China
(associated with Institution Center for High Energy Physics, Tsinghua University, Beijing, China)
[64]School of Physics and Technology, Wuhan University, Wuhan, China
(associated with Institution Center for High Energy Physics, Tsinghua University, Beijing, China)
[65]Institute of Particle Physics, Central China Normal University, Wuhan, Hubei, China
(associated with Institution Center for High Energy Physics, Tsinghua University, Beijing, China)
[66]Departamento de Fisica, Universidad Nacional de Colombia, Bogota, Colombia (associated with Institution LPNHE, Université Pierre et Marie Curie, Université Paris Diderot, CNRS/IN2P3, Paris, France)
[67]Institut für Physik, Universität Rostock, Rostock, Germany (associated with Institution Physikalisches Institut, Ruprecht-Karls-Universität Heidelberg, Heidelberg, Germany)
[68]National Research Centre Kurchatov Institute, Moscow, Russia (associated with Institution Institute of Theoretical and Experimental Physics (ITEP), Moscow, Russia)
[69]Instituto de Fisica Corpuscular, Centro Mixto Universidad de Valencia - CSIC, Valencia, Spain
(associated with Institution ICCUB, Universitat de Barcelona, Barcelona, Spain)
[70]Van Swinderen Institute, University of Groningen, Groningen, Netherlands
(associated with Institution Nikhef National Institute for Subatomic Physics, Amsterdam, Netherlands)

[a]Also at Università di Ferrara, Ferrara, Italy
[b]Also at P.N. Lebedev Physical Institute, Russian Academy of Science (LPI RAS), Moscow, Russia.
[c]Also at Università di Milano Bicocca, Milano, Italy.
[d]Also at Università di Modena e Reggio Emilia, Modena, Italy.
[e]Also at Novosibirsk State University, Novosibirsk, Russia.
[f]Also at LIFAELS, La Salle, Universitat Ramon Llull, Barcelona, Spain.
[g]Also at Università di Bologna, Bologna, Italy.
[h]Also at Università di Roma Tor Vergata, Roma, Italy.
[i]Also at Università di Genova, Genova, Italy.
[j]Also at Scuola Normale Superiore, Pisa, Italy.
[k]Also at Università di Cagliari, Cagliari, Italy.
[l]Also at Università di Bari, Bari, Italy.
[m]Also at Laboratoire Leprince-Ringuet, Palaiseau, France.
[n]Also at Università degli Studi di Milano, Milano, Italy.
[o]Also at Universidade Federal do Triângulo Mineiro (UFTM), Uberaba-MG, Brazil.
[p]Also at AGH - University of Science and Technology, Faculty of Computer Science, Electronics and Telecommunications, Kraków, Poland.
[q]Also at Università di Padova, Padova, Italy.
[r]Also at Iligan Institute of Technology (IIT), Iligan, Philippines.
[s]Also at Hanoi University of Science, Hanoi, Viet Nam.
[t]Also at Università di Pisa, Pisa, Italy.
[u]Also at Università di Roma La Sapienza, Roma, Italy.
[v]Also at Università della Basilicata, Potenza, Italy.
[w]Also at Università di Urbino, Urbino, Italy.